As written, they are endothermic reactions. Yet, each one of them has been found or indicated to proceed easily within zeolites. The most noteworthy aspect common to all of these reactions is that they result in an increase in the number of ions inside the zeolite. We then immediately recall the strongly polarized internal structures of zeolites. As stated earlier, the cations at site II are shielded only on one side. By reason of symmetry, many of the $(AlO_2)^{-1}$ units within the framework must also be shielded unevenly. This polarization would, of course, be more pronounced in zeolites with divalent cations. We should also note that, because of the open network structure of zeolites, the separations between the positively charged regions and the negatively charged regions are large and often encompass the void spaces constituting the channels and cavities. Introduction of additional cations and anions into these void spaces with a proper arrangement should then bring about an increase in the Madelung energy of the crystal. We believe it is this gain in the Madelung energy which offsets the endothermicity of the reaction cited above. Thus zeolites may be viewed as a "solid state electrolytic solvent." Its ionizing power is of such magnitude that not only does it "dissolve" a strong electrolyte such as NaCl in its ionized state, but also accommodates two different molecules A and B in their charge-transfer state, A^+ and B^-. As an extreme example one may cite the formation of Na_4^{3+} centers when Na–Y is treated with Na vapor.[18] The reaction within zeolite can be simply expressed as

$$Na \longrightarrow Na^+ + e^-$$

Catalytic properties of Y-type zeolites for a variety of organic reactions are well known and have been the subjects of many investigations.[22] The observed activity has been attributed to the electric field associated with the cations, to the acidity of the hydroxyl groups incorporated within the structure, or to the combined effect of both. It is quite conceivable that some of these reactions are catalyzed through a charge-transfer state formed as a direct manifestation of the electrolytic property discussed above.

(22) See, for example, a review article by J. A. Rabo and M. L. Poutsma, 2nd International Conference on Molecular Sieve Zeolites, Worcester, Mass., Sept 1970.

Polarized Single-Crystal Absorption Spectra of Pyrazine and Tetramethylpyrazine

Thomas P. Lewis* and Howard R. Ragin

Contribution from the Department of Chemistry, City College of the City University of New York, New York, New York 10031.
Received December 11, 1971

Abstract: Polarized absorption spectra have been measured at room temperature on the (101) crystal face of pyrazine and on the (001) crystal face of tetramethylpyrazine to 2150 Å on a quartz microspectrophotometer. Absolute crystal intensities have been estimated from Lambert's law plots of optical density *vs.* crystal thickness. The absolute intensities and dichroic ratios observed for pyrazine and tetramethylpyrazine crystals are very close to those expected from an oriented gas model of noninteracting molecules and confirm theoretical predictions regarding the polarizations of the first three electric dipole allowed pyrazine singlet–singlet transitions. Second-order dipole–dipole calculations predict the small magnitude of intermolecular effects observed in the crystal spectra.

Although the azabenzenes are a class of polyatomic molecules whose electronic spectra have been investigated in great detail,[1] no reports have appeared in the literature describing the polarized singlet absorption spectra of these compounds in the pure crystalline state. In this paper, we report polarized absorption spectra on single crystals of pyrazine and tetramethylpyrazine measured at room temperature to 2150 Å on a microspectrophotometer. Particular emphasis has been directed in this study toward accurate measurement of absolute crystal intensities so that any intensity modifications caused by intermolecular interactions may be analyzed and interpreted.

There has recently been a good deal of activity devoted to measurement of polarized crystal spectra for heteroaromatic systems of biological interest both by direct absorption[2–5] and by reflection techniques.[6,7] Since a major aim of this work has been the derivation of free-molecule transition moments from linear dichroism measurements, it has been important to assess the extent to which intermolecular interactions in the crystal affect crystal transition intensities and dichroic ratios. Pyrazine is a heteroaromatic system in which free-molecule transition moments are limited by symmetry to three mutually orthogonal directions. Polarized single-crystal spectra may easily distinguish the three alternative polarizations for particular transitions, and deviations of measured intensities from those ex-

(1) K. K. Innes, J. P. Byrne, and I. G. Ross, *J. Mol. Spectrosc.*, 22, 125 (1967).

(2) R. F. Stewart and N. Davidson, *J. Chem. Phys.*, 39, 255 (1963).
(3) W. A. Eaton and T. P. Lewis, *ibid.*, 53, 2164 (1970).
(4) T. P. Lewis and W. A. Eaton, *J. Amer. Chem. Soc.*, 93, 2054 (1971).
(5) M. Tanaka and J. Tanaka, *Bull. Chem. Soc. Jap.*, 44, 672, 938 (1971).
(6) H. H. Chen and L. B. Clark, *J. Chem. Phys.*, 51, 1862 (1969).
(7) P. R. Callis and W. T. Simpson, *J. Amer. Chem. Soc.*, 92, 3593 (1970).

pected by an oriented gas model of noninteracting molecules may be used to assess the influence of intermolecular interactions on the spectra.

The electronic spectrum of pyrazine in the near-ultraviolet consists of absorptions attributable to n → π* and π → π* transitions. Using the axis notation of Innes, Byrne, and Ross,[1] the representations $B_{3u}(x)$, $B_{2u}(y)$, and $B_{1u}(z)$ of the pyrazine molecular point group D_{2h} correspond to electric dipole allowed transitions polarized respectively normal to the pyrazine plane, in-plane perpendicular to the axis of the two nitrogen atoms, and in-plane along the axis of the two nitrogens. The system with electronic origin at about 3300 Å has been assigned as a $^1n\pi^* \leftarrow S_0$ transition,[8-10] and the vapor spectrum in this region displays sharp structure which has been analyzed by Ito, *et al.*[11] Further analysis of the rotational structure of the vapor spectrum under high resolution by Innes and coworkers has revealed that all strong vibronic bands of the 3300-Å system may be accounted for by one electronic transition.[12,13] The absorption in the region 3300–2900 Å consists of sharp bands with x polarization expected for an electric dipole allowed n → π* transition ($^1B_{3u} \leftarrow {}^1A_{1g}$) and weaker broader bands with z polarization. The weaker band system gains intensity through Herzberg–Teller vibronic coupling with an allowed $^1B_{1u} \leftarrow {}^1A_{1g}$ transition. Although observation of an electric dipole forbidden $^1B_{2g} \leftarrow {}^1A_{1g}$ transition has been reported about 450 cm^{-1} to the red of the $^1B_{3u} \leftarrow {}^1A_{1g}$ origin,[14] the assignment is regarded as only provisional by Innes, Byrne, and Ross.[1] It may be noted that a $^1B_{2g} \leftarrow {}^1A_{1g}$ transition is still electric dipole forbidden by the site group symmetry in the pyrazine crystal. A pure crystal spectrum of the 3300-Å system with unpolarized light at 4.2°K has also been measured by Zalewski,[15] but no analysis has been attempted.

The vapor spectra of the pyrazine π → π* systems with origins at about 2700 and 1960 Å are diffuse, and no polarization information may be derived.[1,16] These π → π* transitions are generally identified with the first two singlet π → π* transitions of benzene. The orbital origins of these absorptions have been assigned on the basis of numerous theoretical calculations,[17-22] and they are $^1B_{2u} \leftarrow {}^1A_{1g}$ and $^1B_{1u} \leftarrow {}^1A_{1g}$ for the 2700- and 1960-Å systems, respectively. In this present work, we provide the first experimental verification of these assignments.

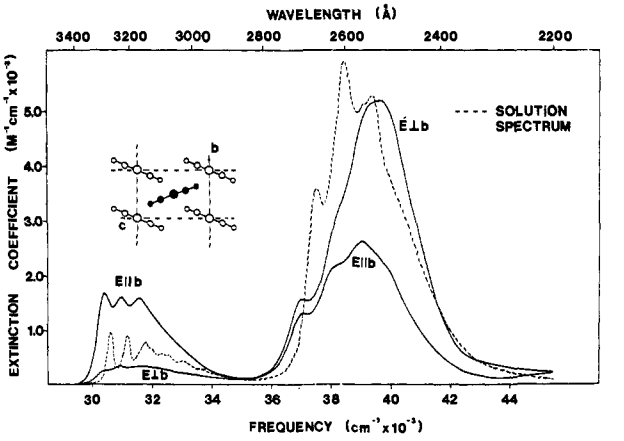

Figure 1. Polarized absorption spectrum of the pyrazine single crystal with light incident normal to the (101) crystal face. Also shown is a solution spectrum of pyrazine in hexane and a projection of the pyrazine crystal structure onto the (100) crystal face. The pyrazine crystal has two molecules per unit cell with crystallographic coordinates (0,0,0) and $(1/2,1/2,1/2)$. These are indicated respectively in the figure as molecules with atoms shown as unshaded and shaded circles, and they will be referred to as crystal sites 1 and 2.

Tetramethylpyrazine retains the D_{2h} molecular point group symmetry of pyrazine but displays a somewhat modified absorption spectrum. The effect of the methyl substitution is to shift the n → π* band to higher energy and the π → π* bands to lower energy. Although the $^1B_{1u} \leftarrow {}^1A_{1g}$ transition in pyrazine is at too high energy to be observed with our microspectrophotometer, in tetramethylpyrazine this transition is shifted to lower energy and is accessible for measurement.

Crystal Structures

Pyrazine crystallizes in the orthorhombic space group *Pmnn* with two molecules per unit cell.[23] Crystals are invariably twinned around (101), and our measurements have undoubtedly been performed on twinned crystal samples (*vide infra*). The unit cell dimensions are a = 9.316 Å, b = 3.815 Å, and c = 5.911 Å, and the concentration in the crystal is, therefore, 15.80 mol/l. A projection of the crystal structure onto the (100) crystal plane is shown in Figure 1. The *N–N* axis of the planar pyrazine molecules coincides with the a crystal axis, and the molecular planes are tilted 22° 3′ around a. The pyrazine site group symmetry is C_{2h}, and there can be no crystal field induced mixing of B_{1u} with either B_{2u} or B_{3u} molecular states.

Tetramethylpyrazine crystallizes in the orthorhombic space group *Pbca* with four molecules per unit cell and unit cell dimensions a = 8.35 Å, b = 9.27 Å, and c = 10.62 Å.[24] The concentration in the crystal is 8.08 mol/l., and the molecules excluding hydrogen atoms are planar. A projection of the tetramethylpyrazine unit cell onto the (001) crystal face is shown in Figure 2.

Crystal Preparation

Pyrazine (99+%, Gold Label) was purchased from Aldrich Chemical Co., Milwakuee, Wis., and was further purified by repeated sublimation over P_2O_5. Tetra-

(8) F. Halverson and R. Hirt, *J. Chem. Phys.*, 17, 1165 (1949).
(9) J. W. Sidman, *Chem. Rev.*, 58, 689 (1958).
(10) M. Kasha, *Discuss. Faraday Soc.*, 9, 14 (1950).
(11) M. Ito, R. Shimada, T. Kuraishi, and W. Mizushima, *J. Chem. Phys.*, 26, 1508 (1957).
(12) K. K. Innes, J. Merrit, W. Tincher, and S. G. Tilford, *Nature (London)*, 187, 500 (1960).
(13) K. K. Innes, J. D. Simmons, and S. G. Tilford, *J. Mol. Spectrosc.*, 11, 257 (1963).
(14) M. A. El Sayed and G. W. Robinson, *Mol. Phys.*, 4, 273 (1961).
(15) E. F. Zalewski, Jr., Ph.D. Thesis, University of Chicago, 1968.
(16) J. E. Parkin and K. K. Innes, *J. Mol. Spectrosc.*, 15, 407 (1965).
(17) See ref 1 for a listing of theoretical calculations performed on the azabenzene $^1\pi\pi^*$ states. Most of these calculations deal only with the π electrons including some more recent treatments.[18,19] Other recent calculations include all-valence-electron semiempirical calculations[20,21] as well as *ab initio* treatments.[22]
(18) R. L. Flurry, Jr., E. W. Stout, and J. J. Bell, *Theor. Chim. Acta*, 8, 203 (1967).
(19) G. W. Pukanic, D. R. Forshey, J. D. Wegener, and J. B. Greenshields, *ibid.*, 10, 240 (1968).
(20) R. Hoffman, *J. Chem. Phys.*, 40, 2745 (1964).
(21) J. Del Bene and H. H. Jaffe, *ibid.*, 48, 1807 (1968).
(22) M. Hackmeyer and J. L. Whitten, *ibid.*, 54, 3739 (1971).
(23) P. J. Wheatley, *Acta Crystallogr.*, 10, 182 (1957).
(24) D. T. Cromer, A. J. Ihde, and H. L. Ritter, *J. Amer. Chem. Soc.*, 73, 5587 (1951).

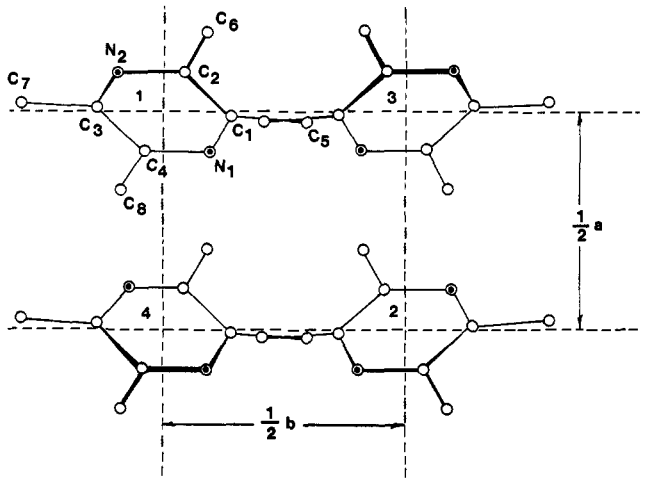

Figure 2. Projection of the unit cell of tetramethylpyrazine onto the (001) crystal plane. The molecules are numbered according to the site designations used in this paper.

methylpyrazine was synthesized according to the method of Kipping[25] and was further purified by distillation and repeated sublimation. The pure compound melts sharply at 86°.

Crystal samples were prepared from melts between ordinary quartz slides and coverslips. Sections of uniform thickness and of high optical quality were used for all measurements. Thicknesses of the order of 0.05–6 μ were required for spectra (see Figures 3 and 4). The high vapor pressure of pyrazine and to a lesser extent of tetramethylpyrazine made it necessary to measure spectra immediately after preparation of samples.

The predominant crystal faces obtained from pyrazine and tetramethylpyrazine melts are (101) and (001), respectively. The face identification is unambiguous for tetramethylpyrazine but must be regarded as somewhat more tentative for pyrazine. For tetramethylpyrazine, X-ray precession photographs were obtained on samples produced from melts or as sublimation flakes (displaying the same face as obtained from the melt) mounted between two thin No. 0 glass coverslips. The zero level photographs yielded the lattice spacings and systematic absences appropriate for the (001) face of tetramethylpyrazine. For X-ray examination of both pyrazine and tetramethylpyrazine, the two coverslips were sealed together with clay or wax, and exposures of as long as 48 hr were obtained without appreciable evaporation of the crystals.

The zero level X-ray precession photographs on pyrazine melts were not of the quality of those obtained on tetramethylpyrazine. The short lattice distances limit the number of reflections that may be observed, and systematic absences occur for $h + k + l = 2n + 1$. The only zero level reflections observed were at distances corresponding to the (020) plane, so there was no doubt that the b axis lay in the crystal plane obtained from the melt. Hochstrasser and Lin have reported that (101) is a cleavage plane of the crystal.[26] These authors have also assumed a unique twinning of the pyrazine crystal around (101), and this was consistent with their results on the polarizations of the factor group components of the lowest pyrazine singlet–triplet transition in a magnetic field. We tentatively identify our crystal face from the melt as (101), and this also proves to be completely consistent with our spectral results. The crystals are twinned around (101) although it should be noted that it is impossible to determine by X-ray crystallography whether pyrazine exists in a twinned unit cell with (101) a common plane to both twins or whether the twinning is random about (101) with some unit cells twinned and others untwinned. This crystal face obtained from the melt gives a centered interference figure under the polarizing microscope which is either an optic normal or obtuse bisectrix figure.

Microspectrophotometer

The microspectrophotometer is similar to one previously described[3] and was constructed with the aid of Mr. Hubert Baxter of Kramer Scientific Co., New York, N. Y. The present instrument has been improved to allow measurement to 2150 Å in the ultraviolet. All measurements were made as previously described.[3] As before, the main virtue of the instrument is its ability to measure high optical densities because of low stray light achieved through use of a double monochromator and double optical masking of the crystal. Spectra were constructed from points generally measured at 5-Å intervals. All spectra were duplicated on at least ten crystals of varying thicknesses. No reflection corrections were made to the observed optical densities. Previous estimates of reflection corrections for crystals displaying absorptions of comparable intensities indicate that reflection corrections for our spectra will never exceed 0.05 absorbance unit.[2-4,27]

Intensities

Crystal thicknesses were estimated from the relationship $t = \Gamma/\Delta n$ where t is the thickness of the crystal, Γ is the relative retardation of the crystal, and Δn is the birefringence of the crystal face. Refractive indices were measured using oil immersion methods. (Refractive index oils were purchased from R. P. Cargille Labs., Inc., Cedar Grove, N. J.) Both pyrazine and to a lesser extent tetramethylpyrazine are dissolved by some of the refractive index liquids. The solubility in the lower index oils ($n < 1.55$) was limited and did not appreciably affect the refractive indices of the liquids. The refractive indices of the higher index oils, however, were significantly affected by the solubility of the crystals. It was necessary to work with refractive index oils saturated with pyrazine or tetramethylpyrazine to measure the higher refractive indices. The indices of the saturated oils were determined using a Bausch and Lomb Abbe-3L refractometer or a Fisher refractometer (Fisher Scientific Co.). Although the refractive indices on the (001) face of tetramethylpyrazine were accurately determined, there was some uncertainty in the value of the higher index for the (101) face of pyrazine. The values measured at 5893 Å for the (101) face of pyrazine and the (001) face of tetramethylpyrazine are: pyrazine, $n_b = 1.466 \pm 0.002$, $n_{\perp b} = 1.670 \pm 0.040$; tetramethylpyrazine, $n_a = 1.539 \pm 0.001$, $n_b = 1.671 \pm 0.002$.

(25) F. B. Kipping, *J. Chem. Soc.*, 2889 (1929).
(26) R. M. Hochstrasser and T. S. Lin, *J. Chem. Phys.*, 53, 2676 (1970).
(27) R. F. Stewart, Ph.D. Thesis, California Institute of Technology, 1963, Appendix A.

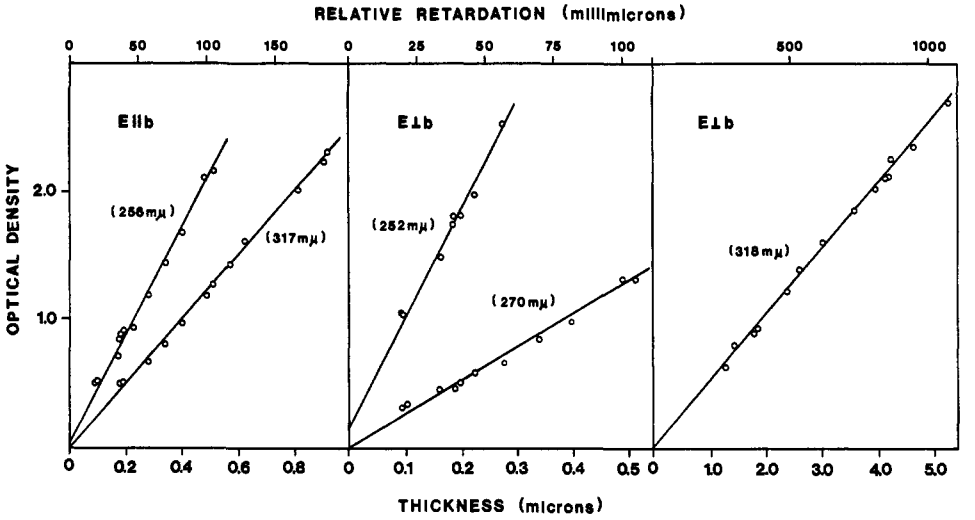

Figure 3. Lambert's law for light incident on the (101) crystal face of pyrazine. Plots of optical density *vs.* crystal thickness for light polarized parallel and perpendicular to the *b* crystal axis. The crystal thickness is calculated from the measured birefringences and relative retardations at 5893 Å. The measured relative retardations are also shown in the figure. Optical densities were measured parallel and perpendicular to the *b* axis at the wavelengths indicated.

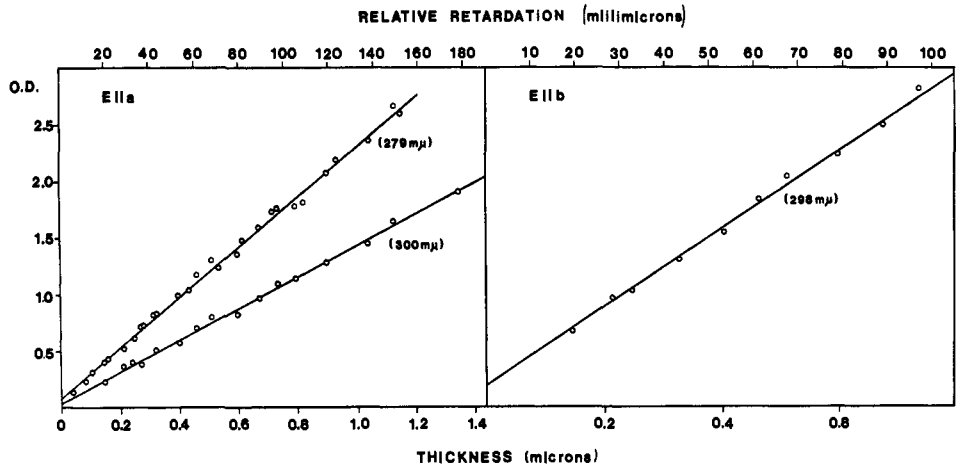

Figure 4. Lambert's law for light incident on the (001) face of tetramethylpyrazine. Plots of optical density *vs.* crystal thickness for light polarized parallel to the *a* and *b* crystal axes. The crystal thickness is calculated from the measured birefringences and relative retardations at 5893 Å. The measured relative retardations are also shown in the figure. Optical densities were measured along the *a* and *b* axes at the wavelengths indicated.

Relative retardations were measured at 5893 Å using a Leitz four-order tilting compensator. In Figures 3 and 4 are shown plots of optical density *vs.* crystal thickness for pyrazine and tetramethylpyrazine crystals. The points were measured at wavelengths in regions of peak or constant absorption. The plots are straight lines which extrapolate to optical densities close to zero for zero crystal thickness.

The slopes of the Lambert's law plots are proportional to crystal molar extinction coefficients. The extinction coefficients calculated from the slopes of the best least-squares lines through the points are: pyrazine, ϵ_b(3170 Å) = 2860 M^{-1} cm^{-1}, ϵ_b (2560 Å) = 4620 M^{-1} cm^{-1}, $\epsilon_{\perp b}$ (3180 Å) = 590 M^{-1} cm^{-1}, $\epsilon_{\perp b}$ (2700 Å) = 2795 M^{-1} cm^{-1}, $\epsilon_{\perp b}$ (2520 Å) = 9400 M^{-1} cm^{-1}; tetramethylpyrazine, ϵ_b (2980 Å) = 7090 M^{-1} cm^{-1}, ϵ_a (3000 Å) = 2810 M^{-1} cm^{-1}, ϵ_a (2790 Å) = 4510 M^{-1} cm^{-1}. It should be noted that both the pyrazine 252-mμ ($\perp b$) and the tetramethylpyrazine 298-mμ lines ($\| b$) extrapolate to intercepts of slightly less than 0.2 at zero crystal thickness. Part of the nonzero intercept may be attributable to our neglect of reflection corrections. Including all sources of experimental error, we estimate 10% to be the maximum uncertainty in our crystal extinction coefficients for tetramethylpyrazine and 25% to be the maximum uncertainty in crystal extinction coefficients for pyrazine.

Results and Discussion

Pyrazine Spectra. The crystal spectrum of pyrazine for light polarized parallel and perpendicular to the *b* crystal axis on the (101) crystal face is shown in Figure 1 together with a solution spectrum of pyrazine in hexane and a projection of the crystal structure onto the (100) crystal face. In Figure 5 is shown an expanded trace of the 3300-Å system, and spectral data for pyrazine are summarized in Table I. Although our crystal samples are twinned, the (101) plane is common to both twins, and our interpretation of spectral

Table I. Spectral Data for Pyrazine[a]

System	Solution in hexane		Crystal $\perp b$ axis		Crystal $\parallel b$ axis		Dichroic ratio	
	$\bar{\nu}_{max}$, cm^{-1}	f	$\bar{\nu}_{max}$, cm^{-1}	f	$\bar{\nu}_{max}$, cm^{-1}	f	$f_{\perp b}/f_b$	$f_b/f_{\perp b}$
$^1B_{3u}$	30,620	0.0014	30,400	0.00055	30,400	0.0040		7.2
	31,175	0.0016	30,930	0.00066	30,965	0.0038		5.7
	31,775	0.0017	31,490	0.00072	31,560	0.0039		5.4
	32,350	0.0014	~32,000	0.00061				
	33,000	0.0012	~32,500	0.00054				
	33,550	0.00059	~33,000	0.00046				
	~34,100	0.00049	~33,550	0.00042				
	~34,600	0.00023	~34,125	0.00029				
	Total	0.0086	Total	0.0046	Total	0.0192		4.2
$^1B_{2u}$	37,520	0.0135	37,025	0.0061	37,020	0.0048	1.3	
	38,460	0.0256	38,175		~38,200			
	39,375	0.0218	39,525		39,040			
	~40,350	0.0106			~40,000			
	~41,300	0.0078						
	Total	0.0794	Total	0.075	Total	0.040	1.9	

[a] The oscillator strength of each band was obtained through graphical integration using the relation $f = 4.32 \times 10^{-9} \int \epsilon d\bar{\nu}$ where ϵ is the decadic molar extinction coefficient and $\bar{\nu}$ is the frequency in units of cm^{-1}.

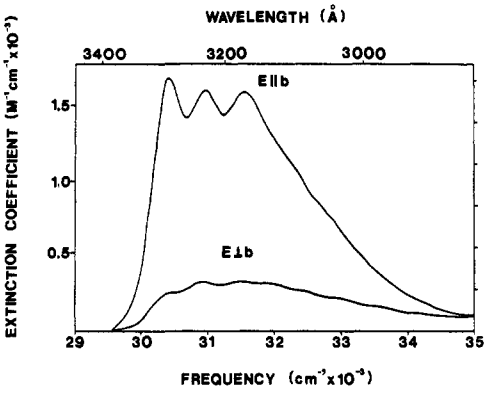

Figure 5. Polarized absorption spectrum of the 3300-Å system of the pyrazine single crystal with light incident normal to the (101) crystal face.

data obtained with light incident normal to the (101) face shall not be greatly complicated by the twinning.

In the oriented gas model of noninteracting molecules, dichroic ratios and intensities are not influenced by intermolecular interactions and can simply be calculated from the known crystal structure. For the pyrazine crystal structure with light incident normal to the (101) face, the dichroic ratio $f_b : f_{\perp b}$ should be 20.3:1.00 for a transition polarized along the pyrazine x direction (B_{3u}) and 1.00:1.67 for a y-polarized transition (B_{2u}). The z direction coincides with the a crystal axis and only projects on the direction $\perp b$ on the (101) face. Moreover, the isolated molecule and crystal intensities should follow the relationship

$$f_{iso} = {}^1/_3(f_a + f_b + f_c)$$

where f_{iso} is an isotropic oscillator strength, which we approximate by the hexane solution oscillator strength.

The observed dichroic ratios listed in Table I for the 3300-Å band system are in reasonable agreement with the $^1B_{3u} \leftarrow {}^1A_{1g}$ assignment. The dichroic ratio ($b : \perp b$) decreases somewhat through the band system and is always lower than the predicted oriented gas value. If one assumes that all of the solution intensity is derived from an x-polarized transition, the predicted oriented gas oscillator strengths parallel and perpendicular to the b axis on the (101) face are 0.022 and 0.0011. These compare with experimental values of 0.019 and 0.0046. The intensity perpendicular to b is almost certainly enhanced by vibrationally induced intensity. The Herzberg–Teller component observed in the vapor spectrum of the 3300-Å system is "borrowed" from an allowed $^1B_{1u} \leftarrow {}^1A_{1g}$ transition and should appear with 84% of its intensity perpendicular to the b axis in our spectrum on the (101) crystal face. Our polarization data allow us to estimate the magnitude of the vibrationally induced component. Assuming the oriented gas model, the anisotropic oscillator strength for the forbidden component is about 0.004, and it accounts for about 15% of the absorption in the band system. The bulk of the forbidden intensity undoubtedly appears in the higher energy part of the absorption and is probably responsible for the difference in band shape between the b and $\perp b$ spectra.

The crystal spectrum like the solution spectrum is characterized by a progression in a symmetric ring breathing mode (ν'_{6a}).[28,29] Although observation of Davydov splittings is difficult at room temperature, it has been possible to make qualitative estimates of the band splittings for the 3300-Å system. Because of considerable overlapping of broad bands, the maxima listed in Table I do not necessarily correspond to the peaks of the individual vibronic bands. The three well-resolved b-axis maxima seem to be at slightly higher energy than their counterparts perpendicular to b. Our estimates of the splittings for the three bands are 0–75 cm^{-1} for the first band, 25–75 cm^{-1} for the second band, and 50–100 cm^{-1} for the third band with the b-axis factor group state always at higher energy.[30]

The 2700-Å $\pi \rightarrow \pi^*$ absorption system as expected appears more strongly perpendicular to the b axis on the (101) face. The dichroic ratio ($f_{\perp b} : f_b$) and absolute intensities are in excellent agreement with those pre-

(28) Innes, Byrne, and Ross[1] have summarized the vibrational modes excited in pyrazine electronic transitions. The assignments and numbering of the normal modes are those of Lord, Marston, and Miller.[29]

(29) R. C. Lord, A. L. Marston, and F. A. Miller, *Spectrochim. Acta*, 9, 113 (1957).

(30) The estimates of the Davydov splittings were made from spectra measured at 2-Å intervals with 150-μ slits on the monochromator. Spectra were measured simultaneously parallel and perpendicular to the b crystal axis on crystals lying close to one another on the microscope slide.

Table II. Spectral Data for Tetramethylpyrazine[a]

System	Solution in hexane		Crystal *b* axis		Crystal *a* axis		Dichroic ratio
	$\bar{\nu}_{max}$, cm^{-1}	*f*	$\bar{\nu}_{max}$, cm^{-1}	*f*	$\bar{\nu}_{max}$, cm^{-1}	*f*	f_b/f_a
$^1B_{3u}$	~34,025	~0.02	~33,550	~0.021	33,250	0.017	~1.2
$^1B_{2u}$	35,990	0.127	35,830	0.199	35,900	0.039	5.10
$^1B_{1u}$	46,950	~0.135					~1.7

[a] Same as for Table I.

dicted by the oriented gas model for a $^1B_{2u} \leftarrow {}^1A_{1g}$ promotion. For the total band system, the predicted oriented gas oscillator strengths are 0.058 ($E \perp b$) and 0.035 ($E \| b$) compared to the observed values of 0.075 and 0.040. The shoulders at about 37,025 cm^{-1} in both polarizations are almost certainly the two components of the O–O band, and they correspond to one another well within our experimental frequency uncertainty. The dichroic ratio in the region of the O–O band is about 1.3 to 1.0, and it increases in the higher energy region of the absorption. The vibrational structure arises from a progression in the symmetric ring breathing mode ν_1, and it is more distinct in the spectrum with light polarized parallel to the *b* crystal axis. The spectrum perpendicular to *b* is more diffuse with some intensity apparently shifted to higher energy. The assignment of the orbital origin of this transition as $^1B_{2u} \leftarrow {}^1A_{1g}$ certainly seems justified beyond doubt by the data.

Tetramethylpyrazine Spectra. Crystal and solution spectra for tetramethylpyrazine are shown in Figure 6. The spectra indicate three distinct electronic transitions, and the spectral data are summarized in Table II. The $^1B_{3u} \leftarrow {}^1A_{1g}$ system has been shifted to higher energy by the methyl substitution and appears to the red of the $^1B_{2u} \leftarrow {}^1A_{1g}$ absorption which has been shifted to lower energy. These shifts are in accord with observed substituent effects on $n \rightarrow \pi^*$ and $\pi \rightarrow \pi^*$ transitions.[31] Both absorption bands are very diffuse, an observation previously reported for the singlet–triplet absorption spectrum of this crystal.[32] The diffuse structure is in accord with a strong perturbation mixing vibronic levels of the overlapping $^1n\pi^*$ and $^1\pi\pi^*$ states.[32] The $^1B_{1u} \leftarrow {}^1A_{1g}$ transition has also been shifted to lower energy and now appears in the high-energy region of the crystal and solution spectra.

Predicted oriented gas *b* to *a* axis dichroic ratios for *x*, *y*, and *z* polarized transitions in tetramethylpyrazine are 1.00:25.5, 3.98:1.00, and 1.34:1.00, respectively. Moreover, intensity for all transitions should also appear along the *c*-crystal axis. Because the $n \rightarrow \pi^*$ transition is strongly overlapped by the more intense $\pi \rightarrow \pi^*$ system, it is difficult to obtain an accurate oscillator strength both for the solution spectrum and for the *b*-axis polarized crystal spectrum. It is immediately obvious, however, that the $n \rightarrow \pi^*$ transition appears much more strongly along the *b* axis than would be predicted by the oriented gas model. The *a*-axis intensity is about as expected, but the *b*-axis intensity is enhanced possibly as a result of crystal field induced mixing with the overlapping $\pi \rightarrow \pi^*$ system.

The $^1B_{2u} \leftarrow {}^1A_{1g}$ transition displays a *b* to *a* polarization ratio quite close to that expected from the oriented gas model. The predicted oriented gas oscillator strengths are 0.195 and 0.049 along *b* and *a* compared to the observed values of 0.199 and 0.039. There is a small hypochromism along the *a* axis, but the polarization ratio and the intensities provide strong support for the $^1B_{2u} \leftarrow {}^1A_{1g}$ assignment.

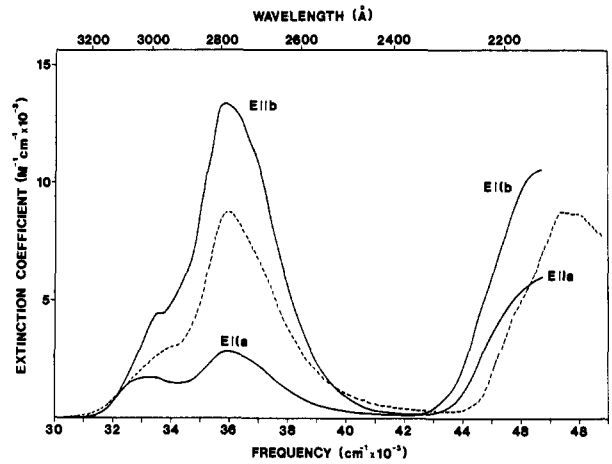

Figure 6. Polarized absorption spectrum of the tetramethylpyrazine single crystal with light incident normal to the (001) crystal face. Also shown is a solution spectrum of tetramethylpyrazine in hexane. The crystal spectra with the electric vector of the incident light parallel to the *a* and *b* crystal axes are shown as solid lines, and the solution spectrum is shown as a dashed line.

Another $\pi \rightarrow \pi^*$ systems begins at about 2300 Å and shows a *b* to *a* dichroic ratio of about 1.7:1.0. This value is in quite good agreement with the predicted oriented gas ratio for a $^1B_{1u} \leftarrow {}^1A_{1g}$ transition. The oriented gas model predicts that 73.5% of the intensity of this *z*-polarized transition should appear on the (001) crystal face, and comparison of solution and crystal spectra in Figure 6 reveals that there is a small hypochromism, primarily along the *a* axis, observed for this absorption.

Discussion

The theoretical assignments of the orbital origins of the first three electric dipole allowed pyrazine transitions are, therefore, confirmed by the crystal spectra. The spectral changes caused by intermolecular interactions are apparently small and do not introduce appreciable error into the derivation of polarization directions for the transitions. The pyrazine and tetramethylpyrazine $^1B_{3u} \leftarrow {}^1A_{1g}$ absorptions both show some deviation from oriented gas behavior. For tetramethylpyrazine, there is extensive overlapping of transitions although it appears that the *b*-axis absorption is enhanced possibly as a result of some crystal field induced mixing with the intense overlapping $\pi \rightarrow \pi^*$ system. The $^1B_{2u} \leftarrow {}^1A_{1g}$ systems of both pyrazine and tetramethylpyrazine show only very small deviations

(31) S. F. Mason, *J. Chem. Soc.*, 1247 (1959).
(32) R. M. Hochstrasser and C. Marzzacco, *J. Chem. Phys.*, **49**, 971 (1968).

from oriented gas intensities. There is a small hyperchromism perpendicular to the *b* axis for pyrazine and a small hypochromism along the *a* axis for tetramethylpyrazine, both of which deviate from oriented gas oscillator strengths by only slightly more than the experimental uncertainty in the spectral intensities.

It is possible to estimate spectral changes caused by intermolecular interactions using well known descriptions for mixing of exciton states in molecular crystals.[33] The crystal Hamiltonian is the sum of molecular Hamiltonians plus coulombic interaction terms. The intermolecular interactions are approximated by a multipole expansion, the first nonvanishing terms being of the dipole–dipole type. These terms remove the degeneracy of the factor group states for a given molecular state in first-order theory (Davydov splittings). In second-order theory, they induce mixing of factor group states of the same symmetry representation corresponding to different molecular excited states. This second effect can lead to modified intensities and dichroic ratios as has been presumed for various other crystal systems.[33,34]

A second-order calculation involves solution of a secular equation for each crystal symmetry type. Lattice sums of dipole–dipole interactions have been evaluated by the Ewald–Kornfeld method and are shown in Tables III and IV for pyrazine and tetramethylpyrazine.

Table III. Dipole Sums for Pyrazine on (101) Crystal Face (in $cm^{-1}/Å^2$)[a-e]

iq	*jr*	$t_{iq,jr}$	$4\pi/v_0(\hat{\mathbf{d}}_{iq}\cdot\hat{\mathbf{k}})(\hat{\mathbf{k}}\cdot\hat{\mathbf{d}}_{jr})$
1*x*	1*x*	−7319	726
1*x*	2*x*	−232	726
1*x*	1*y*	1811	1752
1*x*	2*y*	−507	1752
1*x*	1*z*	0	−2904
1*x*	2*z*	0	−2904
1*y*	1*y*	−1337	4227
1*y*	2*y*	−879	4227
1*y*	1*z*	0	−1203
1*y*	2*z*	0	−1203
1*z*	1*z*	3809	1994
1*z*	2*z*	−5941	1994

[a] *i*, *j* denote unit cell sites designated in Figure 1. [b] *x*, *y*, *z* denote molecular axes as defined in text. [c] $t_{iq,jr}$ are inner dipole sums calculated as described in ref 40. [d] The term $4\pi/v_0(\hat{\mathbf{d}}_{iq}\cdot\hat{\mathbf{k}})(\hat{\mathbf{k}}\cdot\hat{\mathbf{d}}_{jr})$, where v_0 is the volume of the unit cell and $\hat{\mathbf{d}}$ and $\hat{\mathbf{k}}$ represent unit transition moment and wave vectors, is the macroscopic contribution to the dipole–dipole lattice sums as described in ref 40. The total dipole sum $T_{iq,jr}$ is the sum of the inner sum and macroscopic part. [e] Dipole sums have been calculated for an untwinned crystal lattice.

zine.[39] In the case of transitions of moderate intensity ($f \sim 0.1$), dipole–dipole terms should be important, although pyrazine will be treated in the weak coupling approximation, and dipole strengths are reduced to those of the individual vibronic bands. For tetramethylpyrazine, clear vibrational structure is not observed in the spectra, and calculations have been carried out within the strong coupling model. The dipole sums on the (101) face of pyrazine contain a macroscopic part dependent on the orientation of the wave vector of the incident radiation for the spectrum perpendicular to the *b* axis.[40] This macroscopic part is proportional to the product

$$(\hat{\mathbf{d}}_i\cdot\hat{\mathbf{k}})(\hat{\mathbf{k}}\cdot\hat{\mathbf{d}}_j)$$

where $\hat{\mathbf{d}}_i$ and $\hat{\mathbf{d}}_j$ are unit transition moment vectors for sites *i* and *j* of the unit cell and $\hat{\mathbf{k}}$ is a unit vector in the direction of the wave vector. The dipole sums on the (001) face of tetramethylpyrazine contain no macroscopic part since for light incident on a face containing two of the principal axes of an orthorhombic crystal, the wave vector is always orthogonal to the crystal transition moment.

Table IV. Dipole Sums for Tetramethylpyrazine (in $cm^{-1}/Å^2$)[a-c]

i	*j*	$t_{ix,jx}$	$t_{ix,jy}$	$t_{ix,jz}$	$t_{iy,jy}$	$t_{iy,jz}$	$t_{iz,jz}$
1	1	−569	133	146	−481	22	−562
1	2	−1042	−428	106	220	−1320	40
1	3	509	776	591	159	805	35
1	4	−552	−868	−979	−911	−280	−621

[a] *i*, *j* denote unit cell sites designated in Figure 2. [b] *x*, *y*, *z* denote molecular axes as defined in text. [c] $t_{iq,jr}$ are inner dipole sums calculated as described in ref 40.

In the calculation for pyrazine, we have included four electronic transitions including one observed in the vacuum ultraviolet.[16] The first transition has eight vibrational sublevels observed in hexane solution and the second transition has five vibrational sublevels (see Table I). Examination of off-diagonal matrix elements for the second-order calculation immediately reveals that they are *too small* to significantly affect the first-order energies or oriented gas dichroic ratios and intensities. This arises mainly because of the small magnitude of the dipole strengths in the weak coupling case but also because of the relatively small dipole sums connecting electronic states and the large spacings of the states themselves. The calculations for pyrazine, therefore, confirm the small magnitude of crystal field induced intensity changes.

First-order calculated Davydov splittings may be compared to those observed in our spectra for the pyrazine 3300-Å system. The calculated splittings are changed by a maximum of $\sim$0.1 cm^{-1} in the second-order treatment. The calculations predict small splittings of 4, 5, and 5 cm^{-1} for the first three vibronic bands with the factor group state perpendicular to the *b* axis at higher energy. The agreement with the experimental splittings is, therefore, poor, and it should be noted that it is the macroscopic contribution to the lattice sum that places the $\perp b$ state at higher energy.

A feature of our spectra that is explained at least qualitatively by the calculations is the apparent shift of intensity to higher energy in the spectrum perpendicular to the *b* axis for the pyrazine 2700-Å system. The pyrazine *y*-molecular axis makes a large projec-

(33) See, for example, D. P. Craig and S. H. Walmsley, "Excitons in Molecular Crystals," W. A. Benjamin, New York, N. Y., 1968.
(34) See, for example, ref 6, 33, and 35–38 for crystal systems in which second-order treatments have been used with varying success to explain deviations of observed dichroic ratios from oriented gas values.
(35) A. Bree and T. Thirunamachandran, *J. Chem. Soc.*, 397 (1962).
(36) R. M. Hochstrasser, *J. Chem. Phys.*, 40, 2559 (1964).
(37) J. Tanaka, *Bull. Chem. Soc. Jap.*, **38**, 86 (1965).
(38) W. C. Johnson, Jr., and W. T. Simpson, *J. Chem Phys* , **48**, 2168 (1968)
(39) We are grateful to Professor Leigh Clark for providing the computer program used to calculate the lattice sums.
(40) M. R. Philpott, *J. Chem. Phys.*, **50**, 5117 (1969).

tion on the normal to the (101) plane (**k**), and the macroscopic contribution greatly enhances the $\perp b$ lattice sum. The second-order splittings calculated for the five vibronic bands are 214, 399, 342, 168, and 125 cm^{-1} with the $\perp b$ bands at higher energy.[41] In the absence of the macroscopic term, the *b*-axis states would be calculated to be at higher energy. The splittings predict that the spectrum $\perp b$ should be shifted to higher energy and that there should be some merging of bands in the high-energy region. It is evident that the calculations are not in good quantitative agreement with experiment since the experimental splittings are not as large as predicted. Indeed, there is no observed splitting of the O–O band although the higher vibrational bands $\perp b$ are clearly at higher energy. Clark and Philpott have observed the dependence of Davydov splittings on the orientation of the wave vector for spectra measured on several faces of the anthracene crystal.[42] They have noted that calculations of dipole sums in which the macroscopic component is substantial tend to overestimate the band splittings. It is possible that a similar situation obtains in our spectra of the 2700-Å pyrazine system.

We have also carried out calculations on the tetramethylpyrazine spectra. Three electronic transitions with hexane solution energies and intensities listed in Table II were included in our treatment. Again the second-order calculation does not indicate any significant change in oriented gas intensities. In this case although the dipole strengths of the interacting levels are larger, the dipole interactions between inequivalent molecules in the lattice are small, and there is cancellation of contributions from different inequivalent molecules. It should be noted that the apparent enhancement of the *b*-axis $^1B_{3u} \leftarrow {}^1A_{1g}$ absorption observed in the crystal spectrum is not predicted by the calculations. The calculations indicate very small mixing of the $^1B_{3u}$ *b*-axis factor group state with the overlapping $^1B_{2u}$ state and even smaller mixing of *a*-axis factor group states.

Acknowledgments. We gratefully acknowledge the receipt of grants from the City University Faculty Research Program in support of this work. We thank Dr. William A. Eaton for many helpful and stimulating discussions.

(41) The first-order splittings are 217, 410, 351, 170, and 126 cm^{-1} and are, therefore, not greatly changed in the second-order treatment.
(42) L. B. Clark and M. R. Philpott, *J. Chem. Phys.*, **53**, 3790 (1970).

Crystal Nucleation Studies in Supercooled Mesomorphic Phases of Cholesteryl Derivatives[1]

John M. Pochan* and Harry W. Gibson

Contribution from the Xerox Corporation,
Rochester Corporate Research Center, Webster, New York 14580.
Received October 8, 1971

Abstract: Classical nucleation rate theory derived for isotropic systems has been applied for the first time to crystallization from the liquid-crystalline phases of cholesteryl esters and binary mixtures thereof. Interfacial energy parameters are an order of magnitude less in these systems than in normal isotropic systems and are shown to be a function of ester chain length, the type of mesophase, and composition in binary mixtures. Phase diagrams are also determined for binary mixtures.

The study of rate of nucleation or growth of crystals from supercooled liquids has, in the past, yielded important thermodynamic parameters. Studies have been conducted on monomeric and polymeric systems exhibiting liquid and crystal phases.[2,3] The degree of supercooling in pure and mixed mesomorphic systems is unique. Supercooling by as much as 86° for a pure compound has been achieved in this study with the resultant liquid crystal stable to recrystallization for several minutes.

In this paper, we report a unique application of nucleation theory to crystallization from supercooled smectic and cholesteric liquid-crystalline states. In association with this nucleation rate study, phase diagrams of mixed cholesteric systems have been obtained in order to study the effect of one mesomorphic compound or state on another.

Theory

Using transition-state theory, Turnbull and Fisher developed an expression for the rate of homogeneous nucleation in condensed systems.[4] The steady-state nucleation rate per unit volume is given by

$$dn/dt = N_0 \exp(-E_d/RT) \exp(-\Delta F^{\pm}/RT) \quad (1)$$

where E_d is the free energy of activation for transport across a liquid–nucleus boundary; $\Delta F^{\pm}$ is the free energy change associated with nucleus formation, and $N_0 = M_0kT/h$, where M_0 is the number of molecules per unit volume in the liquid, h equals Planck's constant, and k is Boltzmann's constant.

Equation 1 describes nucleation in terms of two different rate processes. At temperatures below the nuclea-

(1) A portion of this work has been previously reported: J. M Pochan and H. W. Gibson, *J. Amer. Chem. Soc.*, **93**, 1279 (1971).
(2) L. Mandelkern, N. J. Jain, and H. Kim, *J. Polym. Sci.*, **6**, 165 (1968).
(3) D. G. Thomas and L. A. K. Stavely, *J. Chem. Soc.*, 4569 (1952).
(4) D. Turnbull and J. C. Fisher, *J. Chem. Phys.*, 17, 71 (1949).